13 Influence of Anterior Chamber Depth, Lens Thickness, and Corneal Diameter on Intraocular Lens Power Calculation

Tiago Bravo Ferreira and Nuno Campos

In this chapter, we will summarize the different intraocular lens (IOL) power calculation formulas, especially those that consider the variables anterior chamber depth (ACD), lens thickness (LT), and/or horizontal corneal diameter (CD), also known as corneal diameter (CD). We will describe the preoperative evaluation of these biometric parameters and their normal values. We will review the influence of each of these three parameters in different IOL power calculation formulas. Finally, highlighting the need for further improvement of refractive results in cataract surgery, we will enumerate future directions for research in this area.

Introduction

In the past decade, cataract surgery transitioned from a replacement of the opacified crystalline lens to a refractive procedure. Residual refractive errors became less frequent, with an increased precision of optical biometry and new IOL power calculation formulas [1].

For spherical IOL power calculation, the combination of optical biometry with last generation formulas such as the Barrett Universal II (BU II) or the Hill-Radial Basis Function (RBF) formulas results in a postoperative refractive result within ±0.50 D of the target in at least 72–84% of the eyes [2, 3], results that still reflect the need for increased precision in IOL power calculation. This is further supported by the knowledge that implantation of new aspheric, multifocal, or toric IOL designs is ineffective unless minimal residual refractive error is achieved [4].

Intraocular Lens Power Calculation Formulas

A number of different mathematical formulas have been proposed to improve postoperative refractive prediction.

These formulas have been subject to several improvements since the first analytical formulas proposed by Fedorov [5], Fyodorov [6], and Colenbrander [7], and the first empirical formula, the SRK, proposed by Sanders, Retzlaff, and Kraff [8, 9]. Analytical formulas rely on a thin lens system to calculate the IOL power, and they all use approximately the same vergence formula.

Given most presently available formulas use non-realistic models for the optics of the eye, they require a number of retrospective corrective factors from observed data in order to work accurately. Therefore, empirical formulas are based on large retrospective populational studies.

The most commonly used empirical formula, the SRK, has been improved with corrective

T. B. Ferreira (✉) · N. Campos
CUF Tejo Hospital, Lisbon, Portugal

J. Aramberri et al. (eds.), *Intraocular Lens Calculations*, Essentials in Ophthalmology,
https://doi.org/10.1007/978-3-031-50666-6_13

factors for extreme eyes and an enhanced algorithm for effective lens position (ELP) estimation, evolving to the SRK II, SRK-T, and, more recently, the SRK-T2 [10]. The effect of these factors is to correct for any off-set errors arising in the formula by applying an average corrective term, making the predictions accurate in the average eye.

In fact, formulas do not account for the actual physical lens position in the pseudophakic eye, but instead use a theoretical position defined as the effective distance from the anterior surface of the cornea to the lens plane as if the lens was of negligible thickness (ELP). This value is provided by the manufacturer as the A-constant is formula-dependent and does not reflect the true ACD in the anatomical sense, which hampers the comparison with postoperative measurements of the pseudophakic ACD, i.e., the postoperative anterior chamber depth (ACD_{post}).

Estimates of postoperative ELP were initially a constant (4 mm). In second-generation formulas, axial length (AL) was introduced as a predictor, and on third-generation formulas, corneal power and AL were used as predictors of postoperative ELP. Given these limitations, and given that the actual postoperative lens position is correlated with AL, ACD, anterior segment depth, and CD [11], new formulas that integrate some or all of the parameters subject of this chapter (ACD, LT, and CD) to predict ELP emerged (Fig. 13.1).

More recent formulas, Holladay 2 (unpublished formula) and Olsen 2 [12], introduce new correlation parameters to compensate for the above-mentioned flaws of third generation formulas. The introduction of more parameters improves the predictive ability of the formulas, decreasing or even removing (Haigis formula) the contribution of the error associated with corneal dioptric power. However, care should be taken with the reproducibility of measuring more parameters and also the fact that regressive factors depend on the measurement technique.

Eyes considered to be average comprise the majority of cases, with the results generally degrading in non-average eyes, due to the statistical nature of the formulas.

Nowadays, multiple formulas exist [13], casting some confusion in clinical practice.

The processing capability of computers no longer requires the simplifications of paraxial optics used nor lengthy population studies. Computerized methods such as artificial intelligence (AI) or ray-tracing emerged as alternatives.

Other new formulas further improved IOL power calculation results by merging the thin lens framework with statistical regression techniques. The main difference between formulas of this type is the variables used and weighting attributed to each one when performing the regression for the ELP value.

New IOL power calculation formulas (Fig. 13.2) include:

- Barrett Universal II (BU II) [14, 15] is a multiple-parameter vergence-based thick-lens formula (although reported to use paraxial ray tracing by Barrett in several personal communications), which has been modified by the author over the years. The formula is unpublished and freely accessible online at calc.apacrs.org/barrett_universal2105/ (accessed March 18, 2021). It uses AL, keratometry (K), and ACD to predict the ELP. Two additional optional parameters may be used, namely LT and CD.
- Emmetropia Verifying Optical (EVO) formula (version 2.0) is a thick-lens formula based on the theory of emmetropization. The formula is unpublished. Version 2.0 of the formula freely accessible online at www.evoiolcalculator.com (accessed March 18, 2021). Predictors of ELP are AL, K, and ACD, with LT and central corneal thickness (CCT) being optional.
- Hill-RBF formula uses AI through a pattern recognition algorithm that considers a form of data interpolation for calculating the IOL power. The Hill-RBF calculator is freely accessible online at www.rbfcalculator.com (accessed March 18, 2021) and also available

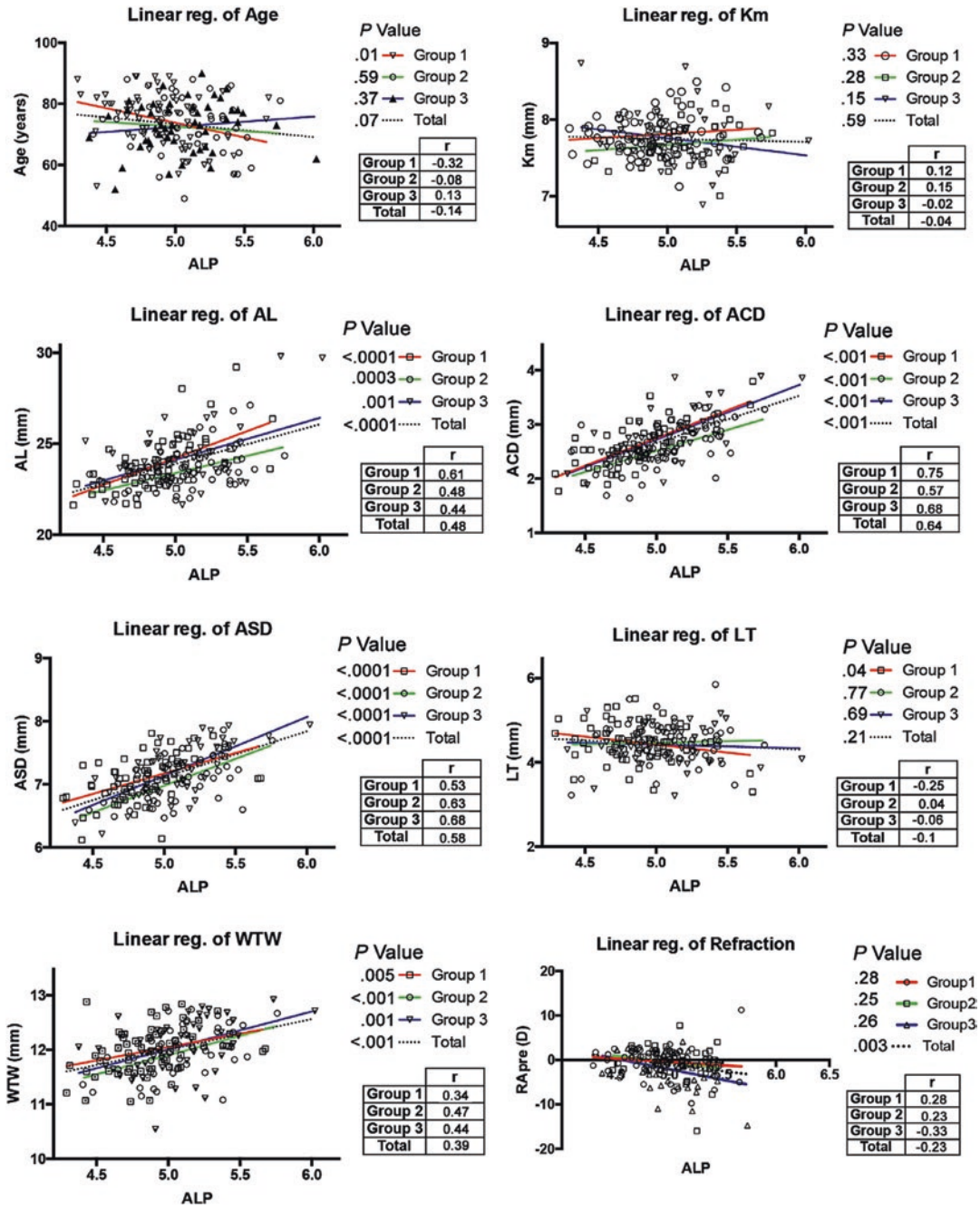

Fig. 13.1 Correlations of actual lens position with age, mean K data, AL, ACD, anterior segment depth, lens thickness, CD distance, and refraction. *ACD* anterior chamber depth, *AL* axial length, *ALP* actual lens position, *ASD* anterior segment depth, *Km* mean keratometry, *LT* lens thickness, *RApre* preoperative refraction assessment, *reg.* regression, *CD* corneal diameter. (Reproduced with permission from J Cataract Refract Surg. 2017 Feb;43(2):195–200)

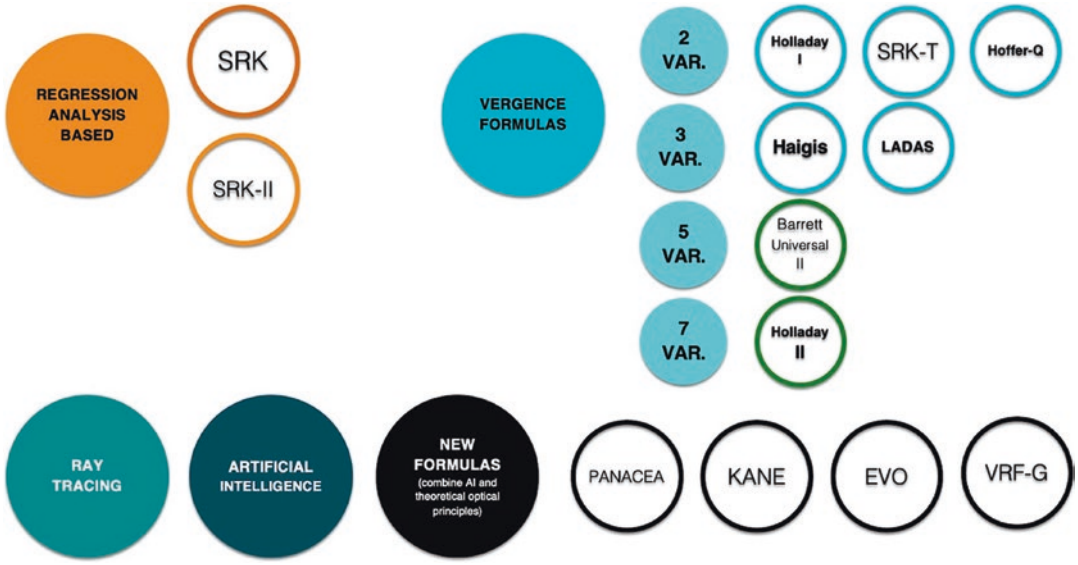

Fig. 13.2 Classification of new intraocular lens power calculation formulas. (Reproduced with permission from Ophthalmology. 2019 Sep;126(9):1334–1335)

on the Lenstar biometer. It is now in version 3.0. AL, K, and ACD are the mandatory data for IOL calculation. LT, CCT, and CD are optional.

– Kane formula is based on a combination of theoretical optics and AI. It is unpublished and freely accessible online at www.iolformula.com (accessed March 18, 2021). The predictors of ELP are AL, K, ACD, and gender. LT and CCT are optional.
– Ladas Super Formula is a combination of the Holladay 1, Holladay 2 (with Wang-Koch adjustment), Hoffer Q, and SRK/T formulas. It is based on a three-dimensional model, adjusting the best formula for a specific eye. The current version of the formula (Ladas Super Formula AI) was developed in 2019. This new version is based on AI and is freely available at www.iolcalc.com (accessed March 18, 2021).
– Næser 2 is a thick-lens formula [16]. It predicts the geometric ACD and not the ELP. The Næser 2 formula, and improvement over the Næser 1 formula, uses calculated data of the IOL architecture and optimized AL measurements to achieve equal results on small, average, and large eyes. The formula is available from its author in Excel (Microsoft Corporation, Redmond, WA, USA).
– Olsen formula was first developed in 1987, undergoing several modifications in the following years [17–19]. The current version is based on ray-tracing [20]. The C constant estimates IOL position based on ACD and LT. The formula can be downloaded at www.phacooptics.net (accessed March 18, 2021). Besides ACD and LT, PhacoOptics software uses four determinants for ELP prediction: AL, K, ACD, and LT. Two versions of Olsen formula are then described: the 4-factor version, also known as $\text{Olsen}_{\text{Standalone}}$ and the 2-factor version, which is installed on optical biometers.
– VRF formula is a vergence based thin-lens formula. The formula is published and uses four variables to predict the ELP (AL, K, ACD, and CD) [21]. The formula is available in its proprietary software (ViOL Commander software v. 2.0.0.0 (V/B/C Systems, Kiev, Ukraine)).
– VRF-G formula is a modification of the VRF formula. The new formula is based on theo-

retical optics, including regression and ray-tracing components. It uses eight variables for ELP prediction (AL, K, ACD, CD, LT, preoperative refraction, CCT, and gender).
– The Prediction Enhanced by ARtificial Intelligence and output Linearization-Debellemanière, Gatinel, and Saad (PEARL-DGS) formula uses machine learning (ML) and output linearization for estimating ELP and calculation the IOL power. It uses adjustments for the biometric values and is unpublished. It is available online at www.iolsolver.com (accessed March 18, 2021).
– T2 formula is an improvement of the SRK/T to circumvent its nonphysiological behavior [10]. It enhances the corneal height calculation of the original formula.

A summary of the constants and metrics used by each formula is presented in Table 13.1.

Table 13.1 Summary of each intraocular lens formula constants and metrics (adapted from Clinical Ophthalmology 2020;14:4395–4402—open access)

Formula	Constants		Metrics
BARRETT UII	LF	2.035	AL, K, ACD, LT, HCD
EVO 2.0	A constant	119.20	AL, K, ACD, LT, CCT
HAIGIS	a0; a1; a2	−0.66; 0.234; 0.217	AL, K, ACD
HILL-RBF 2.0	A constant	119.23	AL, K, ACD
HOFFER Q	pACD	5.75	AL, K
HOLLADAY 1	SF	1.97	AL, K
KANE	A constant	119.18	AL, K, ACD, gender, LT, CCT
NÆESER 2	Korr AL constants	1.43; 0.94	AL, K, ACD
PEARL-DGS	A constant	119.03	AL, K, ACD, LT, HCD, CCT
SRK/T	A constant	119.22	AL, K
T2 FORMULA	A constant	119.22	AL, K
VRF	CACD	5.66	AL, K, ACD, HCD
VRF-G	A constant	119.19	AL, K, ACD, gender, LT, CCT, HCD, preoperative SE

SF surgeon factor, *pACD* personalized anterior chamber depth, *LF* lens factor, *CACD* optical constant of the anterior chamber depth, *AL* axial length, *K* keratometry, *ACD* anterior chamber depth, *LT* lens thickness, *HCD* horizontal cornea diameter, *CCT* central corneal thickness, *SE* refractive spherical equivalent

Performance of Different Formulas

Of all the available formulas, the best performing formulas use more than two parameters for ELP prediction and therefore should be preferred clinically [22].

In two landmark clinical studies [2, 23], Melles et al. investigated the performance of different IOL power calculation formulas. In their second study [23], the authors found Kane formula to be the most accurate, with 84% of the eyes within ±0.50 D of the target. Olsen, BU II, and EVO 2.0 formulas showed the next best results (Fig. 13.3). This was true when both SS-OCT and PCI-based biometers were used to acquire preoperative data.

In a 2016 study [24], Kane et al. reported the BU II to be similarly accurate for both small and long eyes, a finding confirmed in a subsequent study. The formula was superior to Haigis, SRK/T, and T2 formulas for all ALs (Fig. 13.4).

Similar findings were reported by Cooke and Cooke [25] when using the IOLMaster biometer, while the $\text{Olsen}_{\text{Standalone}}$ version was superior to BU II when using the Lenstar biometer. Figure 13.5 depicts two tables with the main study findings.

Shajari et al. [22] also found BU II to be the most precise formula. However, in contrast to the study by Kane et al., the authors found no significant differences between BU II, SRK/T, and T2 formulas. Also, in the study by Shajari et al. [22], differences in mean absolute error (MAE) between Hoffer Q, Holladay 1, and SRK/T formulas were not statistically significant.

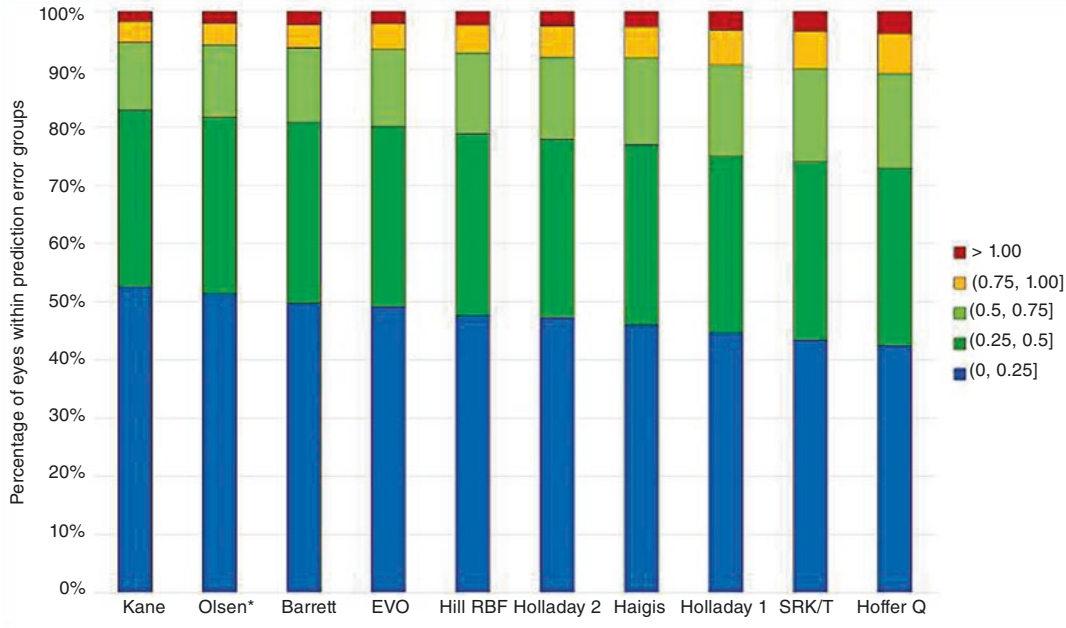

Fig. 13.3 Stacked histogram comparing the percentage of cases within a given diopter range of predicted spherical equivalent refraction outcome for the SN60WF (Alcon Laboratories, Inc., Forth Worth, TX) model intraocular lens. *H1* Holladay 1, *H2* Holladay 2, *HS* Haag-Streit, *WK* Wang-Koch. (Reproduced with permission from Ophthalmology. 2019 Sep;126(9):1334–1335)

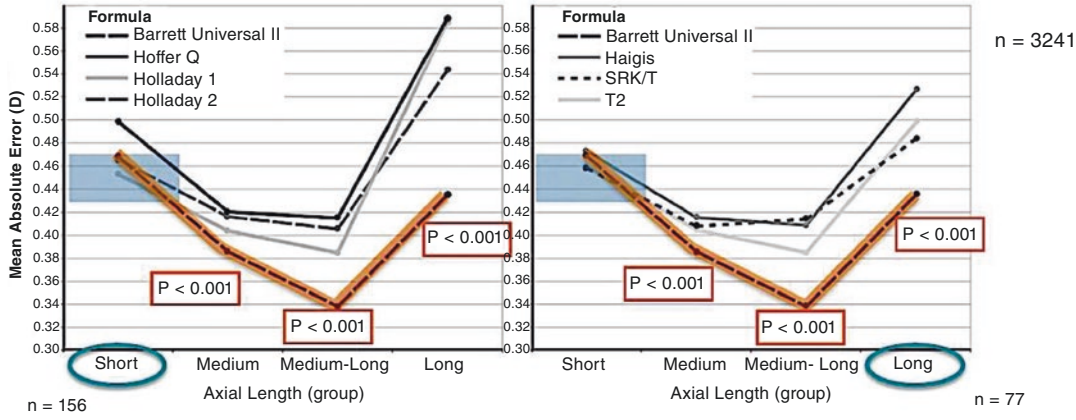

Fig. 13.4 Mean absolute error plotted against AL groups for the Barrett Universal II, Hoffer Q, Holladay 1, Holladay 2, Haigis, SRK/T, and T2 formulas. The formulas are grouped to allow easier visualization. (Adapted with permission from J Cataract Refract Surg. 2016 Oct;42(10):1490–1500)

Table 1. Formula performance for all eyes using optimized lens constants with PCI measurements (mean AL = 23.81 mm; range = 20.87 to 29.44 mm; N = 1079).

Formula	ME (D)	MAE (D)	Med AE(D)	SD	MAX Err	±0.5 D	±1.0D
Barrett	0.00	0.306	0.255	0.387	1.35	80.6	99.3
Haigis*	0.00	0.319	0.271	0.401	1.71	79.8	98.7
T2	0.00	0.319	0.265	0.404	1.70	79.0	98.7
Super Formula	–0.06	0.326	0.275	0.410	1.72	79.9	98.3
Holladay 1*	0.00	0.326	0.270	0.414	1.54	79.5	98.4
Holladay 2_{NoRef}	0.00	0.331	0.287	0.417	1.52	79.3	97.7
Holladay $2_{PreSurgRef}$	0.00	0.346	0.297	0.432	1.47	75.2	98.1
Hoffer Q*	0.00	0.341	0.281	0.432	1.81	77.0	97.4
SRK/T*	0.00	0.346	0.290	0.440	1.89	75.1	98.1
$Olsen_{Standalone}$	0.01	0.348	0.285	0.446	1.59	75.1	97.1

Barrett = Barrett Universal II formula; Holladay 2_{NoRef} = Holladay 2 formula that used all preoperative variables except preoperative refraction; Holladay $2_{PreSurgRef}$ = Holladay 2 formula that used the refraction from the preoperative examination; MAE = mean absolute error; Max Err = maximum prediction error; ME = mean prediction error; Med AE = median absolute error, $Olsen_{Standalone}$ = purchased Olsen formula
*Formulas that were evaluated in a previous study[1]
†Percentage of refractions within ±0.5 D of prediction
‡Percentage of refractions within ±1.0 D of prediction

Table 2. Formula performance for all eyes using optimized lens constants with OLCR measurements (mean AL = 23.81 mm; range = 20.84 to 29.51 mm; N = 1079).

Formula	ME (D)	MAE (D)	Med AE(D)	SD	MAX Err	±0.5 D	±1.0D
$Olsen_{Standalone}$	0.00	0.284	0.225	0.361	1.51	83.7	99.1
Barrett	0.00	0.285	0.230	0.365	1.25	82.9	99.2
$Olsen_{OLCR}$	0.00	0.296	0.245	0.378	1.53	82.0	98.6
Haigis* *	0.00	0.314	0.268	0.393	1.78	80.4	98.7
T2	0.00	0.313	0.262	0.397	1.62	79.6	98.8
Super Formula	–0.06	0.321	0.269	0.403	1.54	79.1	98.4
Holladay 2_{NoRef}	0.00	0.318	0.261	0.404	1.39	79.0	98.1
Holladay 1*	0.00	0.320	0.268	0.408	1.69	79.1	98.6
Holladay $2_{PreSurgRef}$	0.00	0.336	0.288	0.423	1.48	76.6	98.4
Hoffer Q*	0.00	0.340	0.285	0.428	1.66	77.8	97.4
SRK/T*	0.00	0.342	0.289	0.433	1.79	75.7	98.1

Barrett Universal II formula; Holladay 2_{NoRef} = Holladay 2 formula that used all preoperative variables except preoperative refraction; Holladay $2_{PresurgRef}$ = Holladay 2 formula that used the refraction from the preoperative examination; MAE = mean absolute error; Max Err = maximum prediction error, ME = mean prediction error; Med AE median absolute error; $Olsen_{OLCR}$ = preloaded Olsen formula; $Olsen_{Standalone}$ = purchased Olsen formula
*Formulas that were evaluated in a previous study[1]
†Percentage of refractions within ±0.5 D of prediction
‡Percentage of refractions within ± 1.0 D of prediction

Fig. 13.5 Formula performance for all eyes using optimized lens constants with partial coherence interferometry (PCI) measurements (Table 13.1) and optical low coherence reflectometry (OLCR) measurements (Table 13.2). (Reproduced with permission from *J Cataract Refract Surg.* 2016;42:1157–1164)

BU II, EVO 2.0, Kane, and Olsen formulas superiority was confirmed in different studies [26, 27]. A study suggested Kane may be superior in ALs >22 mm [26]. Another study [27] reported similar results for the VRF-G formula when compared with the three other formulas, for eyes of all ALs.

Refractive Prediction Errors after Cataract Surgery

Even if the current formulas offer excellent results, the potential for postoperative ametropia still exists due to pre-, intra-, or postoperative causes. Preoperatively, the current

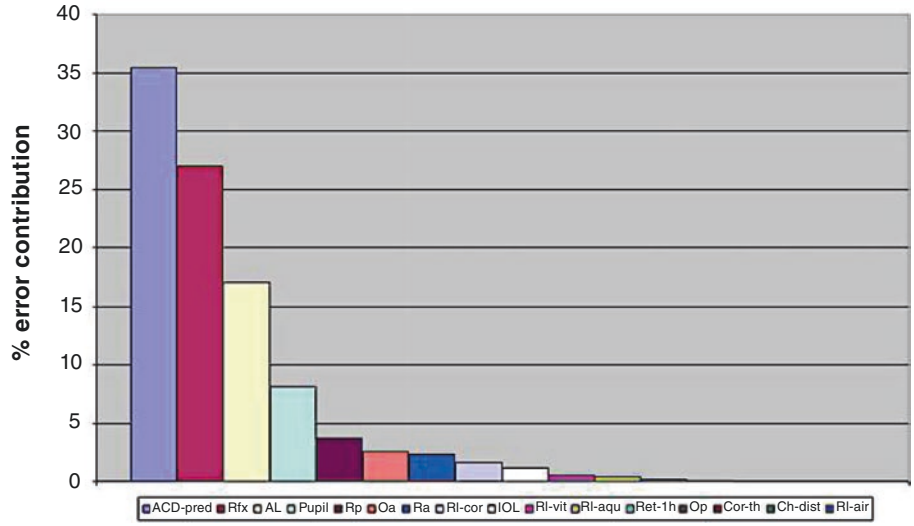

Fig. 13.6 Relative (percentage) error contribution of all factors influencing the refractive outcome of cataract surgery, arranged in order of decreasing magnitude. Eye of average dimensions and properties implanted with a 21.5 D IOL with spherical surfaces. *ACD-pred* prediction of postoperative IOL position, *AL* axial length, *Ch-dist* chart distance, *Cor-th* corneal thickness, *IOL* IOL power, *Pupil* pupil size, *Qa* corneal anterior asphericity, *Qp* corneal posterior asphericity, *Ra* corneal anterior radius, *Ret-th* retinal thickness, *Rfx* postoperative spectacle refraction, *RIair* air refractive index, *RI-aqu* aqueous refractive index, *RIcor* corneal refractive index, *RI-vit* vitreous refractive index, *Rp* corneal posterior radius. (Reproduced with permission from J Cataract Refract Surg 2008;34:368–376)

limitations of biometric data acquisition accuracy and repeatability [28], ocular surface disease [29–31], previous refractive surgery, and ELP prediction limitations should be considered. Our study group showed [32] that, in the phakic eye, AL measurements taken by ultrasound (vitreous chamber depth, LT, and ACD were the most sensitive to biometric errors, with a contribution to the refractive error of 62.7%, 14.2%, and 10.7%, respectively). When optical biometry measurements were considered, postoperative ACD was the most important contributor, followed by the anterior corneal surface and corneal asphericity. A Monte Carlo simulation showed that current limit of refractive assessment is 0.26 D for the phakic eye [32].

It is known that the error in ELP prediction is of major importance to the refractive outcome [33], having a 42% relative contribution to the total refractive error, contrasting with a 36% relative contribution of AL measurement errors and 22% relative contribution of corneal power measurement errors.

Similar values were found by Norrby [28], with the largest contributors of error being estimation of ELP (35%), postoperative refraction determination (27%), and AL measurement errors (17%) (Fig. 13.6).

During surgery, a decentration of the capsulorrhexis of more than 0.4 mm is associated with a 0.25 D change in spherical equivalent (SE) [34]. As our study group showed [35], the surgically induced astigmatism varies significantly, even with fixed incision size and meridian, also contributing to residual refractive error.

Postoperatively, the variability on subjective refraction and shift in IOL position are potential sources of refractive error.

We can conclude that estimation of postoperative IOL position is a major determinant of residual refractive error, hence the importance of considering elements that may improve this estimation in IOL calculation.

Preoperative Evaluation

Accurate biometric measurements are paramount for the correct evaluation of the eye.

Although there are several techniques to measure AL, optically based systems, such as PCI or OLCR, have gained increased popularity in recent years. These systems are more accurate and less dependent on the operator than ultrasound biometry [36–39]. Furthermore, most optical biometers evaluate additional parameters, including corneal curvature, ACD, LT, and CD.

Anterior Chamber Depth

The ACD is an important parameter for IOL power calculation, being used as a variable for ELP prediction in several formulas. ACD can be measured by various techniques:

- A-Scan ultrasound (US)
- Ultrasound biomicroscopy (UBM)
- Optical biometry
- Slit-beam photography
- Scheimpflug imaging
- Anterior segment optical coherence tomography (AS-OCT)

Measurement devices based on these techniques were developed for measuring the ACD. Using them to measure ACD_{post} results in significant discrepancies between measurements obtained with different techniques, being unclear which one is more adequate to accurately measure ACD_{post}. Figure 13.7 demonstrates the concept of ACD measurement pre- and postoperatively.

It is important to note that different measurement techiques have variable agreements between them when evaluating ACD. Thus, their interchangeability should be studied (see topic "Agreement Between Measurement Techniques").

Lens Thickness

US, optical biometry, Scheimpflug photography, and OCT may be used to evaluate LT.

US techniques are more reliable in measuring posterior lens shape in the cataractous eye, whilst OCT [40], or Scheimpflug photography may both be used for analyzing the anterior lens shape. Scheimpflug photography [41] should not be used for posterior lens imaging since the required geometrical distortion induced by the acute angles leads to a significant loss of resolution.

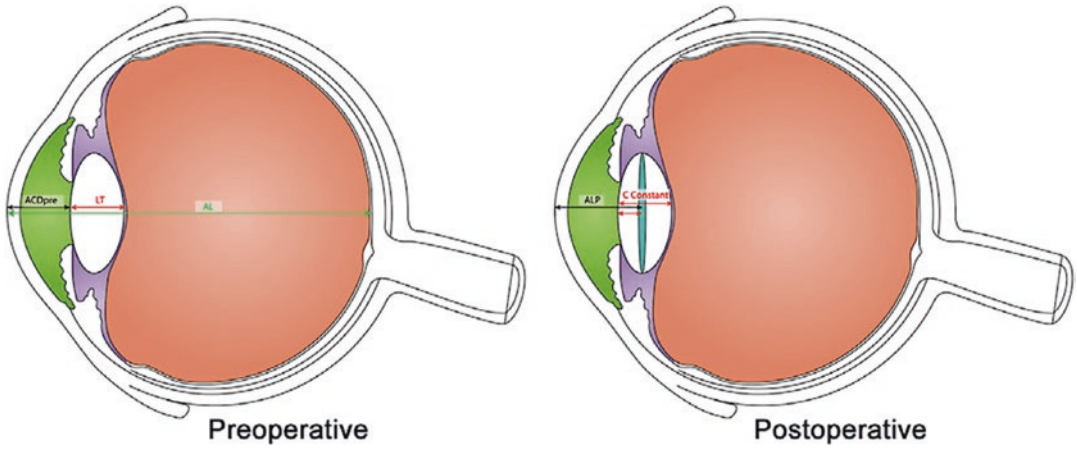

Fig. 13.7 Description of the anterior lens position. *ACDpre* preoperative anterior chamber depth, *AL* axial length, *ALP* actual lens position, *LT* lens thickness. (Reproduced with permission from J Cataract Refract Surg 2017; 43:195–200)

Another technique capable of imaging the cataractous lens shape with high resolution is magnetic resonance imaging (MRI), but the associated costs are still considered too high.

Corneal Diameter

CD can be evaluated using:

- Manual calipers
- UBM
- Digital photography
- Optical biometry
- Corneal topography
- AS-OCT

Definitions of normal CD, as determined by the horizontal CD, are controversial. The generally accepted values of normal horizontal CD of 11.0–13.0 mm are not established by any evidence-based studies, with definitions of microcornea ranging from 10.0 [42–45] to 11.0 mm [46, 47] and of macrocornea from 12.5 [43–46] to 13 mm [48]. It is important to remember that most of these ranges are based on measurements with manual calipers, as automated devices are relatively new.

With any technique, it must be noted that CD measurements are not equivalent to angle-to-angle (ATA) measurements and no accurate prediction of ATA may be derived from CD [48]. When comparing AS-OCT (Visante) with automated CD measurements using the IOLMaster and the Orbscan IIz, a study showed that the internal diameter of the anterior chamber evaluated with AS-OCT is larger than the horizontal CD measured with the other techniques [49].

Agreement Between Measurement Techniques

Repeatability and reproducibility of the above-mentioned techniques are high for most measured parameters. However, agreement is variable. Numerous studies evaluated the agreement between different techniques in the measurement of the biometric parameters topic of this chapter (ACD, LT, and CD).

ACD measurements with the IOLMaster are generally shallower than those of other optical biometers, probably because the slit source that measures ACD is projected from the temporal side, with ACD measured slightly off-center. Sabatino et al. [50] compared two biometers, the IOLMaster and a biometer based on optical low-coherence interferometry (OLCI) in ACD measurement, finding statistically significant differences (3.13 ± 0.36 mm vs. 3.16 ± 0.30 mm, respectively). Repeatability was high for both instruments. On the contrary, Hoffer et al. [51] showed PCI to measure a deeper ACD than OLCR (3.11 ± 0.47 mm vs. 2.98 ± 0.49 mm, respectively; $P < 0.0001$).

When assessing the agreement and comparing ACD measurements between two optical devices (Orbscan II and IOLMaster) and contact US A-Scan, Reddy et al. [52] showed the mean ACD was 3.32 ± 0.60 mm, 3.33 ± 0.61 mm, and 2.87 ± 0.55 mm, respectively ($P < 0.01$). A high agreement between Orbscan II and IOLMaster was noted.

Lee et al. [53] compared ACD measurements (endothelium to anterior capsule of the lens) using the Orbscan IIz and UBM. The authors found a deeper ACD with UBM (2.91 ± 0.43 mm vs. 2.82 ± 0.46 mm, respectively; $P < 0.001$).

Even when using the same technique, differences may still exist. Savini et al. [54] investigated the differences between two Scheimpflug camera devices (Pentacam and Sirius). The mean ACD was 2.90 ± 0.48 mm and 2.94 ± 0.47 mm, respectively. The difference was considered statistically but not clinically significant. Aramberri et al. [55] studied the repeatability, reproducibility, and agreement of the Pentacam HR and a dual-camera Scheimpflug device (Galilei G2) in analyzing the anterior segment. The ACD measurement precision was high, with a within-subject standard deviation (Sw) value of 0.02 mm, and intraclass correlation coefficient (ICC) values higher than 0.993. Other authors [56] showed that the Galilei G4 yielded a significantly shallower ($P < 0.05$) ACD measurement than the Pentacam HR.

One study [57] compared the ACD and CD using the Zeiss Meditec Atlas, IOLMaster 500, Orbscan II, and Pentacam and found the largest agreement to exist between the IOLMaster and the Pentacam.

Baikoff et al. [58] compared a PCI device (IOLMaster 500) with an AS-OCT prototype (Carl Zeiss Meditec). The mean ACD was 3.53 ±0.35 mm with the IOLMaster and 3.64 ±0.33 mm with the AS-OCT. OCT measurements were more reproducible.

When studying OCT biometers, Hoffer et al. [59] showed small differences exist between OLCR and swept-source (SS)-OCT (IOLMaster 700) in ACD measurement (−0.03 mm; $P < 0.001$). Comparing a new SS-OCT biometer (Argos) with the IOLMaster 500 and the Lenstar LS900, Shammas et al. [60] found a difference in ACD of −0.17 ± 0.20 mm for the PCI device, and 0.08 ± 0.15 mm for the OLCR device.

Recently, Tañá-Rivero et al. [61] compared a Scheimpflug-PCI device (Pentacam AXL) with two SS-OCT biometers (IOLMaster 700 and ANTERION). The authors found a statistically significant difference in ACD, LT, and CD between the biometers ($P < 0.001$), with the IOLMaster showing the shallowest and ANTERION the deepest ACD.

In another recent study [62], intraoperative OCT yielded a significantly deeper ACD value than PCI. However, this difference did not reflect a significant difference in IOL calculation using the BU II formula.

Differences between measurement devices should be remembered when using formulas that consider ACD in IOL power calculation.

Savini et al. [63] investigated the differences in LT between immersion US and three optical biometers (OA-2000, Alladin and Galilei G6). Differences were small but statistically significant and influenced IOL selection, resulting, when using the optical biometry measurements, in a selection of a lower power IOL in between 43.2% and 62.5% of eyes, depending on the optical biometer.

In the study by Kurian et al. [64] there were significant differences between OLCR and SS-OCT biometry when evaluating LT (−0.06 mm; $P < 0.001$).

Fisus et al. [65] compared the IOLMaster 700 with a new SS-OCT biometer (ANTERION), finding a difference of and 0.07 ± 0.04 mm in both LT and ACD between both biometers. Although the differences were small, the authors suggested the devices are not interchangeable.

Domínguez-Vicent et al. [66] reported that CD depends not only on image quality but also on the algorithms chosen for limbus detection. Differences in formulas that use CD as a variable, such as Holladay 2 or BU II, may be found. The authors [56] also found that the mean CD was 11.84 ± 0.31 mm and 11.90 ± 0.43 mm when measured with the Galilei G4 and the Pentacam HR, respectively.

It is also known that measurements of CD with the Pentacam HR and the Orbscan IIz are similar [67].

In the study by Tañá-Rivero et al. [61], the IOLMaster showed the largest CD and the Pentacam the shortest (12.00 ± 0.51 mm vs. 11.67 ± 0.51 mm, respectively; $P < 0.001$). The LT measured with IOLMaster was thicker than that measured with ANTERION (4.23 ± 0.57 mm vs. 4.20 ± 0.58 mm, respectively; $P < 0.001$).

A recent metanalysis [68] demonstrated a high agreement between measurements of AL, ACD, and corneal power with the Lenstar and IOLMaster. However, significant differences in CD between the two devices were found (mean difference OLCR to PCI −0.14 mm; 95% CI −0.25 to −0.02 mm; $P = 0.02$).

Thus, significant differences in CD should be considered in the case of formulas that use this parameter for IOL power calculation, the same being true for ACD and LT.

When evaluating these biometric parameters, it is important to remember that pupil dilation causes a significant variation of their values [69–73], with some studies also showing differences in IOL power when using some formulas, particularly BU II [55]. Hence, biometry should always be acquired in the same standard conditions, preferably through an undilated pupil and by the same experienced operator.

Population Means

Given the paucity of published studies of ocular biometric parameters using optical biometry, we recently characterized the ocular biometric parameters and their associations in a population of cataract surgery candidates in Portugal, using the Lenstar LS900 optical biometer [74].

The mean values of ACD, LT, and CD are shown in Table 13.2.

The histograms of the distribution of the ACD, LT, and CD values are shown in Figs. 13.8, 13.9, and 13.10, respectively.

The AL, ACD, LT, and CD were all significantly correlated between each other ($P < 0.001$).

Table 13.2 Demographic data and mean ocular biometric parameters in a Portuguese population

Parameter	Mean ± SD (range)		
Eyes (*n*)	6506		
Patients (*n*)	6506		
Anterior chamber depth (mm) ± SD Range	3.25 ± 0.44 (2.04–5.28)	3.30 ± 0.40 (2.06–5.42)	3.14 ± 0.43 (2.04–4.99)
Lens thickness (mm) ± SD Range	4.32 ± 0.49 (2.73–5.77)	4.35 ± 0.49 (2.75–5.77)	4.38 ± 0.41 (2.73–5.42)
Corneal diameter (mm) ± SD Range	12.02 ± 0.46 (10.50–14.15)	12.03 ± 0.43 (10.51–14.15)	11.98 ± 0.49 (10.50–14.09)

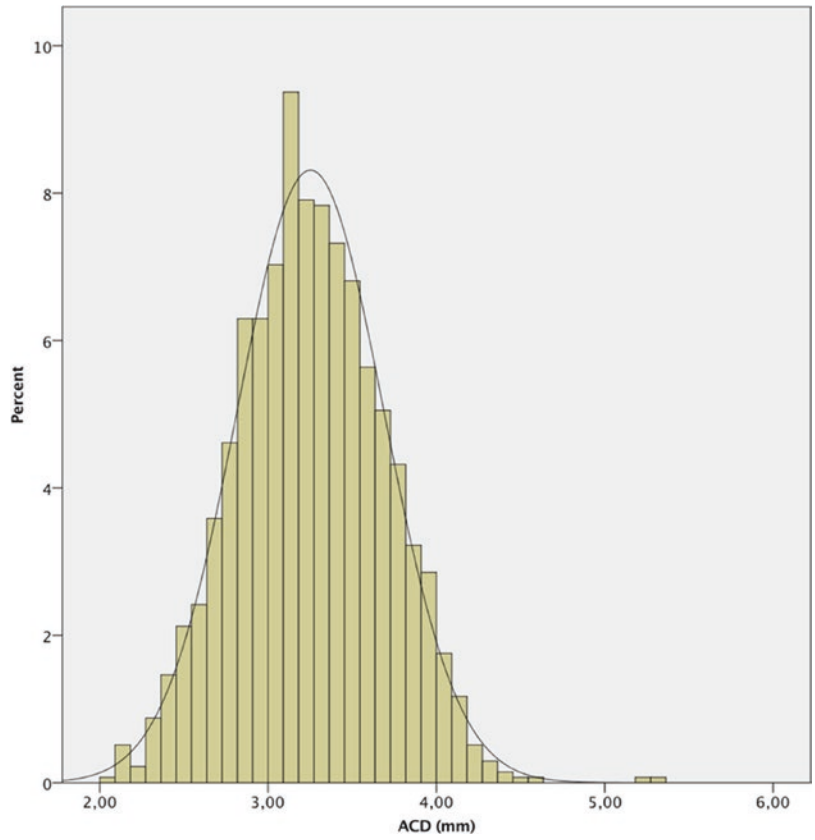

Fig. 13.8 Histogram of anterior chamber depth (ACD) of the study population

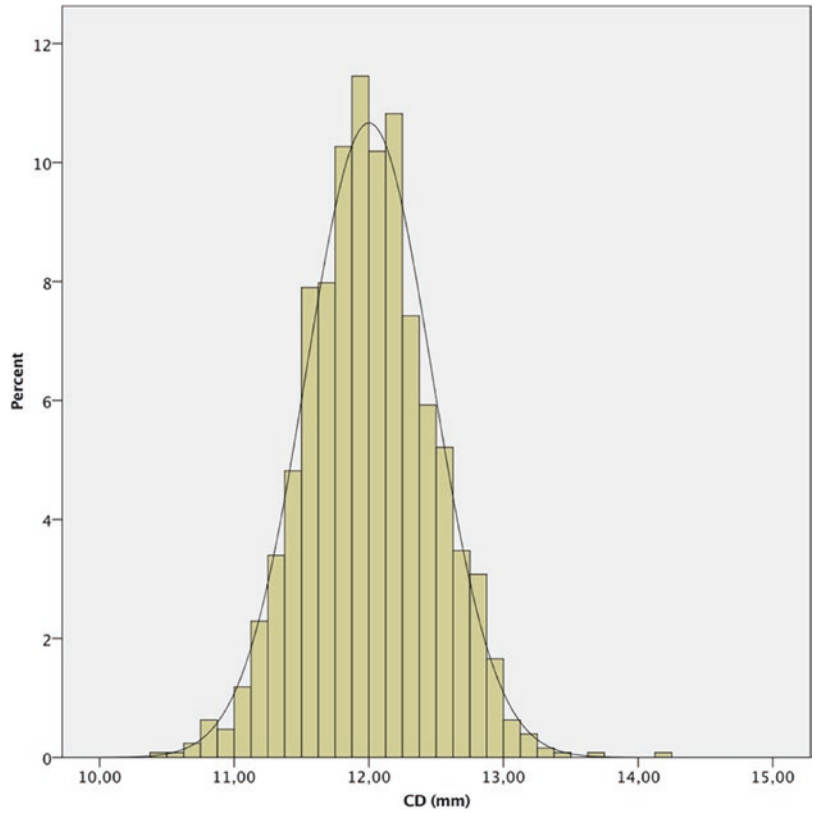

Fig. 13.9 Histogram of corneal diameter (CD) of the study population

The mean ACD in our population (3.25 ± 0.44 mm) was higher than that reported in most studies in Eastern [75–78] and Western populations, and it is comparable with that reported by Hoffer in the USA [79].

The mean LT was 4.32 ± 0.49 mm, and it was directly proportional to age and inversely proportional to AL. These findings confirm those of the studies by Jivrajka et al. [64] and Hoffer [65, 80], although LT in our study was thinner than those studies reported. The mean CD in our study (12.02 ± 0.46 mm) was similar to that reported in other series in the literature [64, 81].

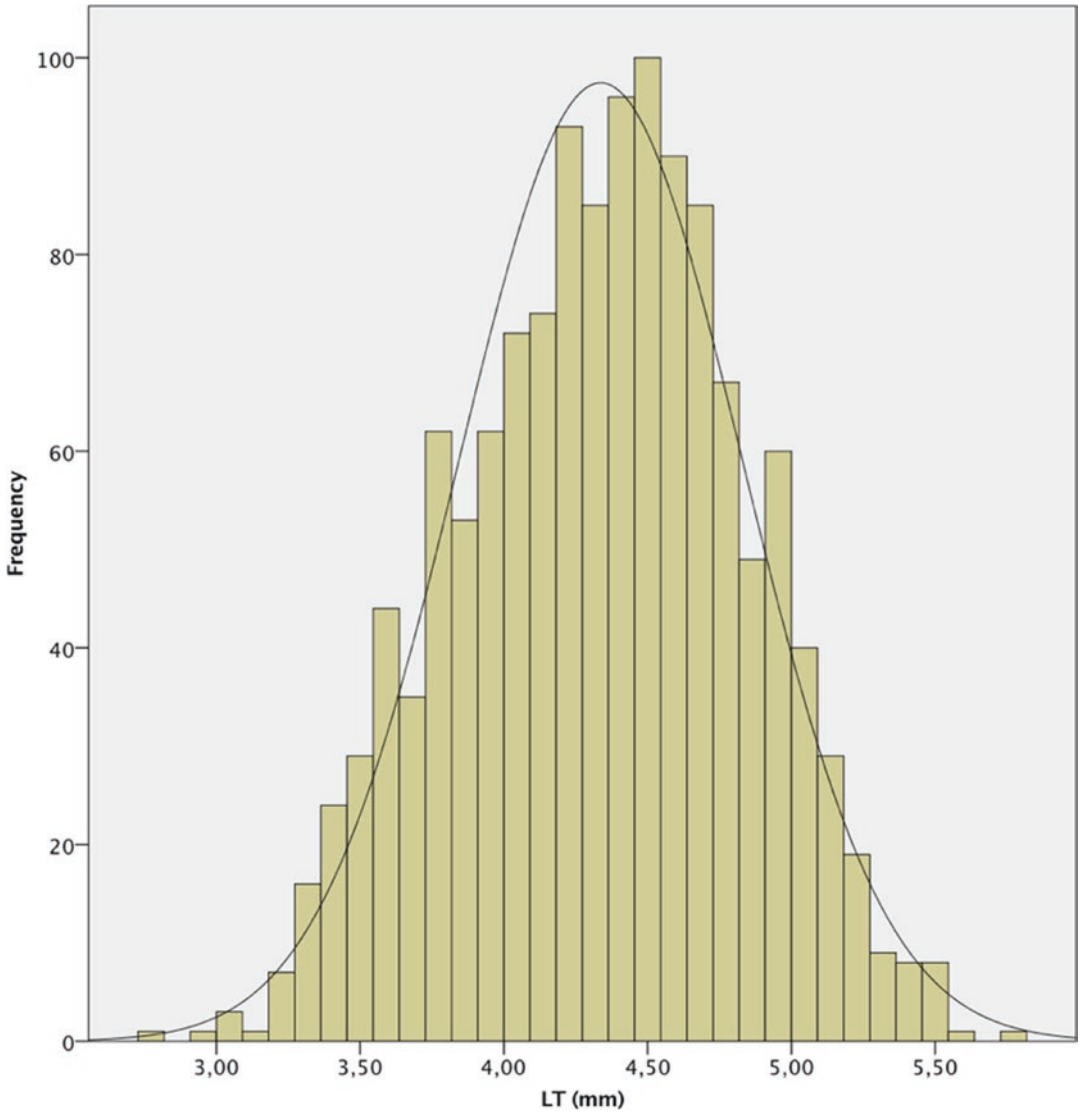

Fig. 13.10 Histogram of lens thickness (LT) of the study population

Influence of Anterior Chamber Depth on Intraocular Lens Power Calculation

It is known that the change in ACD after cataract surgery has an impact on postoperative refractive error (a hyperopic shift will small changes and a myopic shift with larger changes) [82].

Formulas may fail in short eyes and shallow ACDs. Also, there is no agreement on the accuracy of different formulas in long eyes with deep ACDs [2, 83–85].

In a 2013 study, our group evaluated the effect of changes in each optical parameter on the refractive status of the eye [32]. We found that, for each 1% increase in ACD, refractive error changes −0.044 D. Thus, a change of 0.179 mm in ACD is required for a 0.25 D variation in refractive error. If we also consider AL, a change of 0.25 mm in ACD measurement corresponds to

an error of 0.10 D in an eye with an AL of 30.0 mm. This error increases 5 times (to 0.50 D) in an eye with an AL of 20.0 mm. This is the reason because precisely estimating ACD is much more important in short than in long eyes.

It is interesting to note that Savini et al. [13] studied two formulas—(BU II) and EVO 2.0—where ACD is an optional parameter, and results of each of these formulas were better when no ACD was entered. However, the authors point out that errors in ACD measurement may explain the results.

When using the BU II formula [86], the optional variables (ACD, LT, and CD) seem to have the least effect in long eyes (AL ≥26.0 mm) and the greatest effect in short eyes (AL ≤22.0 mm), where clinically significant differences are found, further stressing the importance of the optional parameters in these eyes.

In the study by Melles et al. [2], the relationship between ACD and refractive prediction error was investigated. For Hoffer Q, Holladay 1, and Olsen formulas, there was a significant bias in prediction error with variations in ACD (Fig. 13.11).

In a study of third-generation and Haigis formulas [87], Jeong et al. showed ACD was the key factor for the difference between third-generation formulas and Haigis. Of the third-generation formulas, larger errors with ACD variations were observed with the Hoffer Q than with the SRK-T formula.

Hipólito-Fernandes et al. [88] studied the influence of ACD and LT in the accuracy of five vergence based and four new generation formulas. The authors divided the eyes in three groups, according to ACD. The Vergence-based two-variable formulas (SRK/T, Holladay 1, and Hoffer Q) revealed a significant myopic shift in group 1 (ACD ≤3.00 mm) and a significant hyperopic shift in group 3 (ACD ≥3.50 mm). In group 1, Kane and Hill-RBF v2.0 were better than the other formulas. The same formulas outperformed others in group 2, while in group 3 Hill-RBF performed the best (Fig. 13.12). Kane, PEARL-DGS, EVO 2.0, and BU II had lower MAE, median absolute errors (MedAE), and a higher percentage of eyes within ±0.25 D than the other formulas.

Gökce et al. [70] studied the influence of ACD on nine formulas in eyes with normal ALs. In eyes with ACD ≤3.0 mm or ≥3.5 mm, ACD was an important variable in the accuracy of IOL calculation. In eyes with normal ALs and ACD ≤3.0 mm or ≥3.5 mm, the BU II, Haigis, Holladay 2, and the $\text{Olsen}_{\text{Standalone}}$ formulas performed better than two variable formulas (Hoffer Q and Holladay 1) and the $\text{Olsen}_{\text{OLCR}}$ formula.

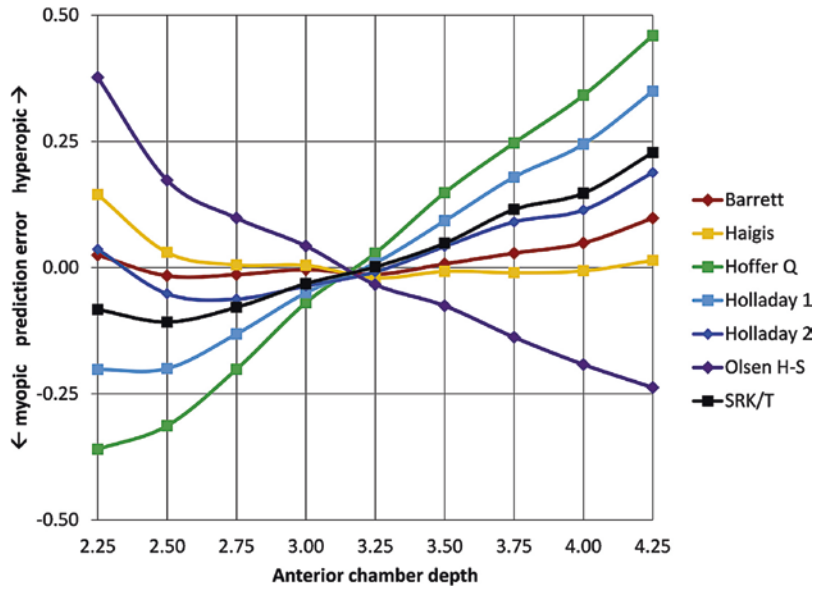

Fig. 13.11 Correlations between anterior chamber depth and postoperative prediction error for different formulas. (Reproduced with permission from Ophthalmology 2018 Feb;125(2):169–178)

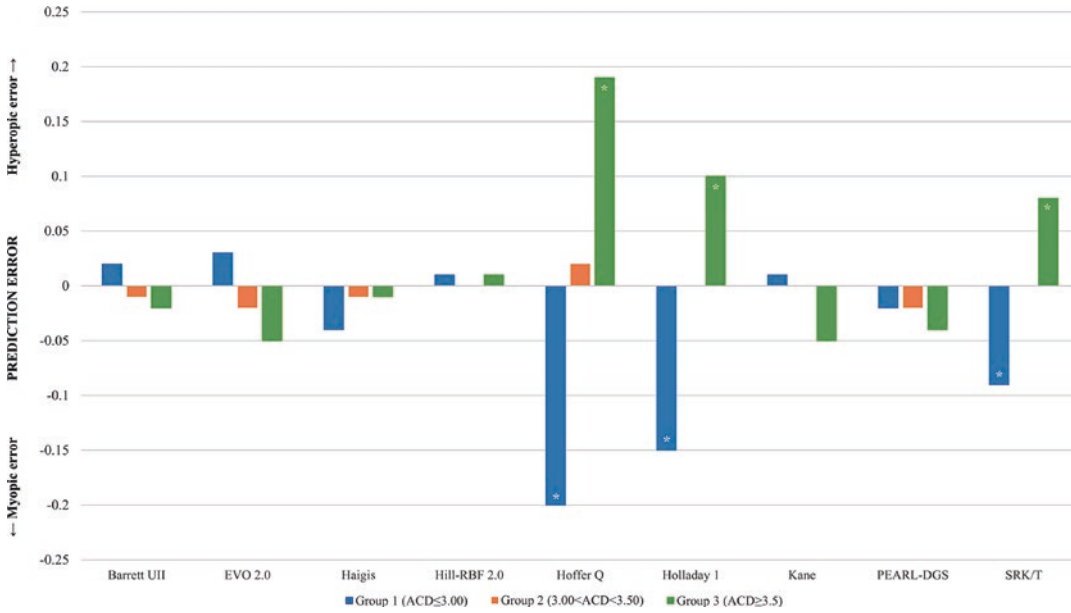

Fig. 13.12 Mean prediction error (in diopters) of each formula, distributed by anterior chamber depth (ACD) group, listed by alphabetic order. *$P < 0.05$—one sample *t*-test. *EVO* emmetropia verifying optical. (Reproduced with permission from Br J Ophthalmol. 2020 Nov 23:bjophthalmol-2020-317822)

The effect of ACD in eyes with different ALs was studied by Yang et al. [85] The Hoffer Q formula was preferred over other formulas in eyes with AL <22.0 mm and ACD <2.5 mm. In eyes with AL <24.5 mm and ACD <2.5 mm, the Haigis formula resulted in myopic refractive prediction errors, while in eyes with AL ≥25.0 mm and ACD ≥3.5 mm it was the preferred formula.

Similarly, Fernandez et al. [89] showed that predictability of different formulas was reduced in eyes with very shallow ACD (ACD ≤2.46 mm). However, in contrast with other studies, and probably due to the low number of eyes in these groups in the study by Fernandez et al., a decrease in accuracy was not found in short eyes or shallow ACD (>2.46 mm).

The accuracy of formulas in short eyes (AL <22 mm) was studied by Shrivastava et al. [90] The performance of seven formulas (BU II, Haigis, Hill-RBF, Hoffer Q, Holladay 1, Holladay 2, and SRK/T) on these eyes was evaluated. In eyes with ACD ≥2.4 mm, Haigis was the best performing formula, with SRK/T being the worst, while in eyes with ACD <2.4 mm, although the differences were not significant, Haigis performed the worst.

Influence of Lens Thickness on Intraocular Lens Power Calculation

Lenticular growth, mainly sagittal, occurs throughout life, and it has been estimated that the equatorial diameter increases about 0.02 mm/year [91]. This thickening occurs predominantly in the anterior direction [92], with the consequent anterior movement of the center of the lens and shallowing of the anterior chamber [93]. This has clear implications on ACD_{post} estimation, given in a younger population a higher lens thickness should correspond to a greater IOL depth, while in an older population, such as a cataract population, a greater lens thickness and smaller IOL depth should be found.

In a study where our group evaluated the effect of changes in each optical parameter on the refractive status of the eye [73], we found that for

each 1% increase in LT refractive error changes −0.097, with a change of 0.104 mm in LT required for a 0.25 D variation in refractive error.

The relationship between different ocular biometric parameters and prediction error of different formulas was studied by Melles et al. [2] When considering LT, Haigis and Holladay 2 were the formulas most affected by its variation (Fig. 13.13).

Similarly, Hipolito-Fernandes et al. [76] found a tendency for a myopic shift with thinner lenses and a hyperopic shift with thicker lenses. This effect was particularly evident for the Haigis and Hill-RBF v2.0 formulas. According to what was shown by Melles et al., BU II had higher prediction errors (hyperopic shifts) with thicker lenses, when compared with the Hoffer Q and Holladay 1 formulas. For the Kane and PEARL-DGS formulas, the MAE was never significantly different from zero across all the LT range (Fig. 13.14).

In another study supporting these findings, Kim et al. [94] showed BU II formula to have the least bias in prediction error according to variations in LT. Refractive errors predicted by the Haigis and Holladay 2 formulas were correlated with LT ($P < 0.001$).

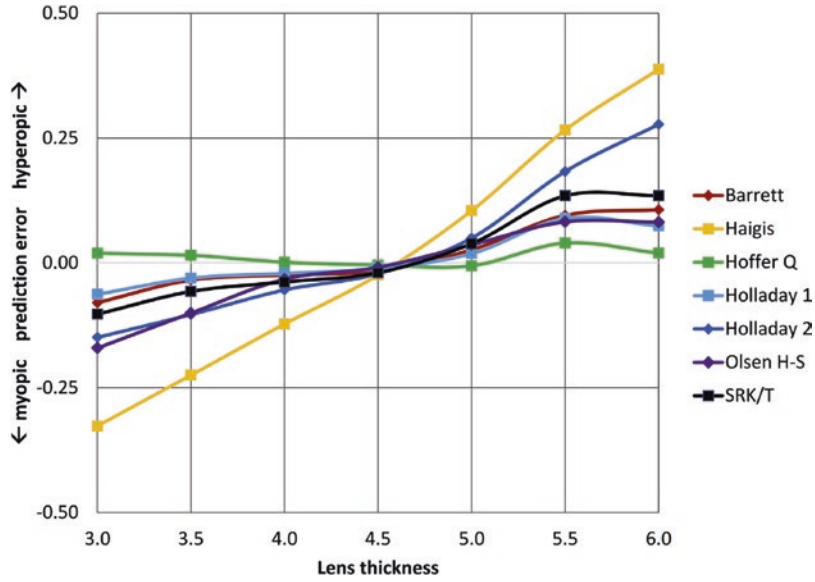

Fig. 13.13 Correlations between lens thickness and postoperative prediction error for different formulas. (Reproduced with permission from Ophthalmology 2018 Feb;125(2):169–178)

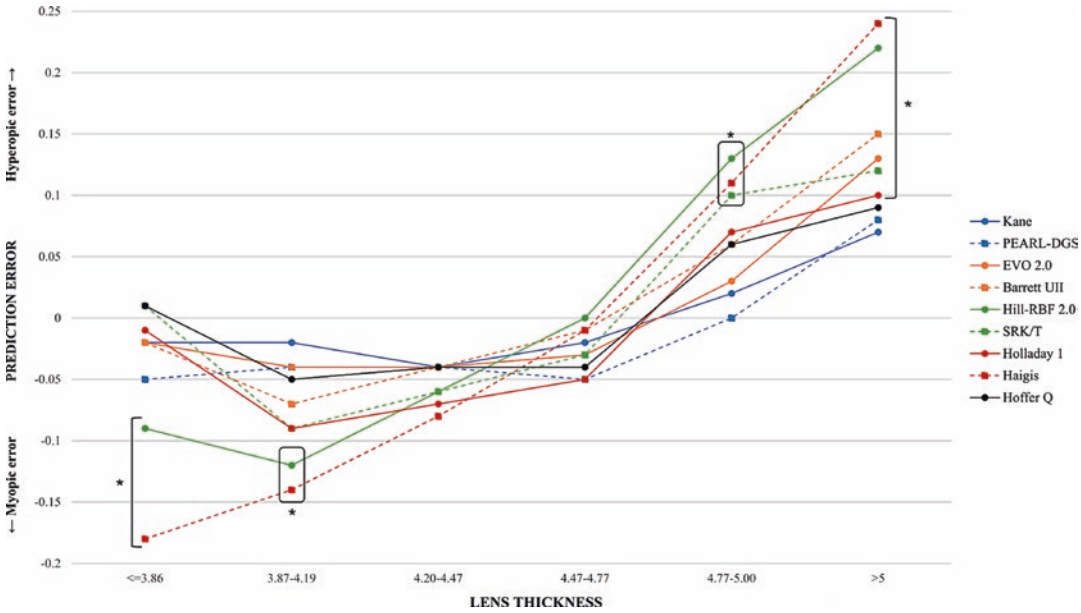

Fig. 13.14 Mean prediction error (in diopters) of each formula, from lens thickness percentile tenth until 90th (in millimeters). *$P < 0.05$—one sample *t*-test. *EVO* emmetropia verifying optical. (Reproduced with permission from Br J Ophthalmol. 2020 Nov 23:bjophthalmol-2020-317822)

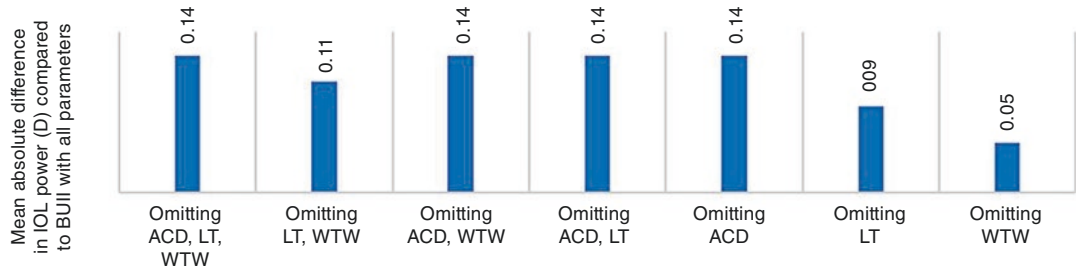

Fig. 13.15 The mean absolute difference in IOL power calculation between partial biometry data and all Barrett Universal II (BUII) parameters in the whole cohort. *ACD* anterior chamber depth, *D* diopters, *IOL* intraocular, *LT* lens thickness, *CD* corneal diameter. (Reproduced with permission from J Clin Med. 2021;10(3):542—open access)

Influence of Corneal Diameter on Intraocular Lens Power Calculation

When studying the influence of optional parameters in BU II, Vega et al. [74] showed that the effect of omitting CD was less than that of omitting ACD or LT (Fig. 13.15), which have more profound and similar effects across all ALs.

The Case of Toric Intraocular Lenses

With the increasing importance of a precise refractive outcome in cataract surgery, accuracy in planning of astigmatic correction also became critical. The classical toric calculators had several limitations in the calculation of the cylindrical power of toric IOLs. Besides not considering the IOL's spherical power or the posterior corneal

surface, it is known that, for each cylindrical power at the IOL plane, a corresponding magnitude of astigmatism is corrected at the corneal plane. This variability depends on the distance between the cornea and the IOL [95, 96]. Most classical toric IOL calculators (e.g., the original toric calculator from Alcon (Alcon Laboratories Inc., Fort Worth, TX, USA)) [97] assumed a fixed ratio (in Alcon's case, 1.46) between the cylindrical power at the corneal and IOL plane. This results in undercorrections in long eyes and overcorrections in short eyes (e.g., in an eye with an axial length of 20.0 mm the real ratio is 1.29 and in an eye with an axial length of 30.0 mm the real ratio is 1.86) [98, 99].

Recently, strategies to overcome this limitation, such as including the ACD and CCT in toric IOL power calculation, were described [100–102].

Future Perspectives

Several paths of investigation aim to improve the main source of error we have identified in this chapter, ELP. These include the use of new imaging techniques or AI strategies.

The use of OCT imaging for improving ELP estimation has been approached by different authors [103]. Goto et al. [104] developed and validated a formula for predicting ACD_{post} from preoperative ATA depth measured by AS-OCT. ATA depth proved to be the most effective parameter for predicting ACD_{post}. Results seem to improve the accuracy of IOL power calculation, with postoperative ACDs of the new formula, the SRK/T formula, and Haigis formulas being predicted with R^2 of 0.71, 0.36, and 0.55, respectively, and the MedAEs being 0.10 mm, 0.65 mm, and 0.30 mm, respectively.

Martinez-Henriques et al. developed an OCT model to improve ELP estimation [105]. The authors obtained a three-dimensional full image of the crystalline lens with quantitative AS-OCT eye imaging. The IOL position after surgery was used to calculate refraction estimation errors. The authors showed that considering the full lens shape is valuable for calculating the ELP.

Satou et al. [106] developed and validated a new method of IOL power calculation based on paraxial ray tracing of the postoperative IOL position captured with AS-OCT. The percentage of eyes within ±0.50 D of the newly developed formula was 84.3% and results showed no correlation with AL or keratometry, which may improve the outcomes in eyes with abnormal proportions.

Different AI strategies for predicting ELP are also being used, namely ML processes. Li et al. [107] showed ACD was the most important input in an ML model, followed by LT, AL, and CD. Subsequently [108], the authors integrated an ML-based method for predicting ELP into existing formulas (Haigis, Hoffer Q, Holladay, and SRK/T) and showed that replacing each of the formulas ELP estimation with the new model improved the performance of all the formulas.

In conclusion, ACD, LT, and CD are important parameters for IOL power calculation and should, in the future, play a primordial role in improving ELP prediction.

Financial Disclosure The author has no proprietary or financial interests in any of the subjects described in this chapter.

References

1. Koch DD, Hill W, Abulafia A, Wang L. Pursuing perfection in intraocular lens calculations: I. Logical approach for classifying IOL calculation formulas. J Cataract Refract Surg. 2017;43(6):717–8.
2. Melles RB, Holladay JT, Chang WJ. Accuracy of intraocular lens calculation formulas. Ophthalmology. 2018;125(2):169–78.
3. Kane JX, Van Heerden A, Atik A, Petsoglou C. Accuracy of 3 new methods for intraocular lens power selection. J Cataract Refract Surg. 2017;43(3):333–9.
4. Hayashi K, Hayashi H, Nakao F, Hayashi F. Influence of astigmatism on multifocal and monofocal intraocular lenses. Am J Ophthalmol. 2000;130:477–82.
5. Fedorov SN, Kolinko AI. A method of calculating the optical power of the intraocular lens. Vestn Oftalmol. 1967;80(4):27–31.

6. Fyodorov SN, Galin MA, Linksz A. Calculation of the optical power of intraocular lenses. Investig Ophthalmol. 1975;14(8):625–8.
7. Colenbrander MC. Calculation of the power of an iris clip lens for distant vision. Br J Ophthalmol. 1973;57(10):735–40.
8. Retzlaff J. Posterior chamber implant power calculation: regression formulas. J Am Intra Ocular Implant Soc. 1980;6(3):268–70.
9. Sanders DR, Kraff MC. Improvement of intraocular lens power calculation using empirical data. J Am Intra-Ocular Implant Soc. 1980;6(3):263–7.
10. Sheard RM, Smith GT, Cooke DL. Improving the prediction accuracy of the SRK/T formula: the T2 formula. J Cataract Refract Surg. 2010;36(11):1829–34.
11. Plat J, Hoa D, Mura F, Busetto T, Schneider C, Payerols A, Villain M, Daien V. Clinical and biometric determinants of actual lens position after cataract surgery. J Cataract Refract Surg. 2017;43(2):195–200.
12. Jin H, Rabsilber T, Ehmer A, Borkenstein AF, Limberger IJ, Guo H, et al. Comparison of ray-tracing method and thin-lens formula in intraocular lens power calculations. J Cataract Refract Surg. 2009;35(4):650–62.
13. Savini G, Di Maita M, Hoffer KJ, Næser K, Schiano-Lomoriello D, Vagge A, Di Cello L, Traverso CE. Comparison of 13 formulas for IOL power calculation with measurements from partial coherence interferometry. Br J Ophthalmol. 2020;105:484. Epub ahead of print.
14. Barrett GD. Intraocular lens calculation formulas for new intraocular lens implants. J Cataract Refract Surg. 1987;13:389–96.
15. Barrett GD. An improved universal theoretical formula for intraocular lens powerprediction. J Cataract Refract Surg. 1993;19:713–20.
16. Næser K, Savini G. Accuracy of thick-lens intraocular lens power calculation based on cutting-card or calculated data for lens architecture. J Cataract Refract Surg. 2019;45(10):1422–9.
17. Olsen T. Theoretical approach to intraocular lens calculation using Gaussian optics. J Cataract Refract Surg. 1987;13:141–5.
18. Olsen T, Corydon L, Gimbel H. Intraocular lens power calculation with an improved anterior chamber depth prediction algorithm. J Cataract Refract Surg. 1995;21:313–9.
19. Olsen T. Prediction of the effective postoperative (intraocular lens) anterior chamber depth. J Cataract Refract Surg. 2006;32:419–24.
20. Olsen T, Hoffmann P. C constant: new concept for ray tracing-assisted intraocular lens power calculation. J Cataract Refract Surg. 2014;40:764–73.
21. Voytsekhivskyy OV. Development and clinical accuracy of a new intraocular lens power formula (VRF) compared to other formulas. Am J Ophthalmol. 2018;185:56–67.
22. Shajari M, Kolb CM, Petermann K, Böhm M, Herzog M, de'Lorenzo N, Schönbrunn S, Kohnen T. Comparison of 9 modern intraocular lens power calculation formulas for a quadrifocal intraocular lens. J Cataract Refract Surg. 2018;44(8):942–8. Erratum in: J Cataract Refract Surg. 2018 Nov;44(11):1409.
23. Melles RB, Kane JX, Olsen T, Chang WJ. Update on intraocular lens calculation formulas. Ophthalmology. 2019;126(9):1334–5. Epub 2019 Apr 11.
24. Kane JX, Van Heerden A, Atik A, Petsoglou C. Intraocular lens power formula accuracy: comparison of 7 formulas. J Cataract Refract Surg. 2016;42:1490–500.
25. Cooke DL, Cooke TL. Comparison of 9 intraocular lens power calculation formulas. J Cataract Refract Surg. 2016;42:1157–64.
26. Cheng H, Kane JX, Liu L, Li J, Cheng B, Wu M. Refractive predictability using the IOLMaster 700 and artificial intelligence-based IOL power formulas compared to standard formulas. J Refract Surg. 2020;36(7):466–72.
27. Hipólito-Fernandes D, Elisa Luís M, Gil P, Maduro V, Feijão J, Yeo TK, Voytsekhivskyy O, Alves N. VRF-G, a new intraocular lens power calculation formula: a 13-formulas comparison study. Clin Ophthalmol. 2020;14:4395–402.
28. Norrby S. Sources of error in intraocular lens power calculation. J Cataract Refract Surg. 2008;34:368–76.
29. Chuang J, Shih KC, Chan TC, Wan KH, Jhanji V, Tong L. Preoperative optimization of ocular surface disease before cataract surgery. J Cataract Refract Surg. 2017;43:1596–607.
30. Holladay JT, Hill WE, Steinmueller A. Corneal power measurements using Scheimpflug imaging in eyes with prior corneal refractive surgery. J Refract Surg. 2009;25:862–8. Erratum in: J Refract Surg 2010;26(6):387.
31. Latkany RA, Chokshi AR, Speaker MG, Abramson J, Soloway BD, Yu G. Intraocular lens calculations after refractive surgery. J Cataract Refract Surg. 2005;31:562–70.
32. Ribeiro F, Castanheira-Dinis A, Dias JM. Refractive error assessment: influence of different optical elements and current limits of biometric techniques. J Refract Surg. 2013;29(3):206–12.
33. Olsen T. Sources of error in intraocular lens power calculation. J Cataract Refract Surg. 1992;18(2):125–9.
34. Okada M, Hersh D, Paul E, van der Straaten D. Effect of centration and circularity of manual capsulorrhexis on cataract surgery refractive outcomes. Ophthalmology. 2014;121:763–70.
35. Ferreira TB, Ribeiro FJ, Pinheiro J, Ribeiro P, O'Neill JG. Comparison of surgically induced astigmatism and morphologic features resulting from femtosec-

ond laser and manual clear corneal incisions for cataract surgery. J Refract Surg. 2018;34(5):322–9.
36. Binkhorst RD. The accuracy of ultrasonic measurement of the axial length of the eye. Ophthalmic Surg. 1981;12:363–5.
37. Seres A, Németh J, Süveges I. Unexpected ametropia after intraocular lens implantation: the role of different factors of ultrasound biometry and surgery. Doc Ophthalmol Proc Ser. 1997;61:415–20.
38. Drexler W, Findl O, Menapace R, et al. Partial coherence interferometry: a novel approach to biometry in cataract surgery [letter]. Am J Ophthalmol. 1998;126:524–34.
39. Kiss B, Findl O, Menapace R, et al. Refractive outcome of cataract surgery using partial coherence interferometry and ultrasound biometry. Clinical feasibility study of a commercial prototype II. J Cataract Refract Surg. 2002;28:230–4.
40. Zeng Y, Liu Y, Liu X, Chen C, Xia Y, Lu M, He M. Comparison of lens thickness measurements using the anterior segment optical coherence tomography and A-scan ultrasonography. Invest Ophthalmol Vis Sci. 2009;50(1):290–4.
41. Wegener A, Laser-Junga H. Photography of the anterior eye segment according to Scheimpflug's principle: options and limitations—a review. Clin Exp Ophthalmol. 2009;37:144–54.
42. Leibowitz HM, et al. Corneal disorders: clinical diagnosis and management. 2nd ed. Philadelphia: Saunders; 1998. p. 204–6.
43. Rapuano C, et al. Anterior Segment. St. Louis: Mosby, Inc.; 2000. p. 47–9.
44. Smolin G, et al. The cornea. 3rd ed. Little, Brown; 1994. p. 538–9.
45. Khng C, Osher RH. Evaluation of the relationship between corneal diameter and lens diameter. J Cataract Refract Surg. 2008;34:475–9.
46. Albert DM. Albert & Jakobiec's principles & practice of ophthalmology. 3rd ed. Philadelphia: Elsevier Inc.; 2008.
47. Arffa RC. Diseases of the cornea. 4th ed. St Louis: Mosby; 1997. p. 86.
48. Piñero DP, Plaza Puche AB, Alió JL. Corneal diameter measurements by corneal topography and angle-to-angle measurements by optical coherence tomography: evaluation of equivalence. J Cataract Refract Surg. 2008;34(1):126–31.
49. Kohnen T, Thomala MC, Cichocki M, Strenger A. Internal anterior chamber diameter using optical coherence tomography compared with white-to-white distances using automated measurements. J Cataract Refract Surg. 2006;32(11):1809–13.
50. Sabatino F, Findl O, Maurino V. Comparative analysis of optical biometers. J Cataract Refract Surg. 2016;42(5):685–93.
51. Hoffer KJ, Shammas HJ, Savini G. Comparison of 2 laser instruments for measuring axial length. J Cataract Refract Surg. 2010;36(4):644–8. https://doi.org/10.1016/j.jcrs.2009.11.007. Erratum in: J Cataract Refract Surg. 2010 Jun;36(6):1066.
52. Reddy AR, Pande MV, Finn P, El-Gogary H. Comparative estimation of anterior chamber depth by ultrasonography, Orbscan II, and IOLMaster. J Cataract Refract Surg. 2004;30(6):1268–71.
53. Lee JY, Kim JH, Kim HM, Song JS. Comparison of anterior chamber depth measurement between Orbscan IIz and ultrasound biomicroscopy. J Refract Surg. 2007;23(5):487–91.
54. Savini G, Carbonelli M, Sbreglia A, Barboni P, Deluigi G, Hoffer KJ. Comparison of anterior segment measurements by 3 Scheimpflug tomographers and 1 Placido corneal topographer. J Cataract Refract Surg. 2011;37(9):1679–85.
55. Aramberri J, Araiz L, Garcia A, Illarramendi I, Olmos J, Oyanarte I, Romay A, Vigara I. Dual versus single Scheimpflug camera for anterior segment analysis: precision and agreement. J Cataract Refract Surg. 2012;38(11):1934–49.
56. Domínguez-Vicent A, Monsálvez-Romín D, Aguila-Carrasco AJ, García-Lázaro S, Montés-Micó R. Measurements of anterior chamber depth, white-to-white distance, anterior chamber angle, and pupil diameter using two Scheimpflug imaging devices. Arq Bras Oftalmol. 2014;77(4):233–7.
57. Hsu M, Christiansen SM, Moshirfar M. Comparison of white-to-white horizontal corneal diameter and anterior chamber depth using the atlas, IOLMaster, Orbscan II, and Pentacam instruments. ARVO annual meeting abstract, Mar 2012.
58. Baikoff G, Jitsuo Jodai H, Bourgeon G. Measurement of the internal diameter and depth of the anterior chamber: IOLMaster versus anterior chamber optical coherence tomographer. J Cataract Refract Surg. 2005;31(9):1722–8.
59. Hoffer KJ, Hoffmann PC, Savini G. Comparison of a new optical biometer using swept-source optical coherence tomography and a biometer using optical low-coherence reflectometry. J Cataract Refract Surg. 2016;42(8):1165–72.
60. Shammas HJ, Ortiz S, Shammas MC, Kim SH, Chong C. Biometry measurements using a new large-coherence-length swept-source optical coherence tomographer. J Cataract Refract Surg. 2016;42(1):50–61.
61. Tañá-Rivero P, Aguilar-Córcoles S, Tello-Elordi C, Pastor-Pascual F, Montés-Micó R. Agreement between two swept-source OCT biometers and a Scheimpflug partial coherence interferometer. J Cataract Refract Surg. 2020;47:488.
62. Muniz Castro H, Tai AX, Sampson SJ, Wade M, Farid M, Garg S. Accuracy of intraocular lens power calculation using anterior chamber depth from two devices with Barrett universal II formula. J Ophthalmol. 2019;2019:8172615.

63. Savini G, Hoffer KJ, Schiano-Lomoriello D. Agreement between lens thickness measurements by ultrasound immersion biometry and optical biometry. J Cataract Refract Surg. 2018;44(12):1463–8.
64. Kurian M, Negalur N, Das S, Puttaiah NK, Haria D, Tejal SJ, Thakkar MM. Biometry with a new swept-source optical coherence tomography biometer: repeatability and agreement with an optical low-coherence reflectometry device. J Cataract Refract Surg. 2016;42(4):577–81.
65. Fișuș AD, Hirnschall ND, Findl O. Comparison of two swept-source optical coherence tomography-based biometry devices. J Cataract Refract Surg. 2021;47:87.
66. Dominguez-Vicent A, Pérez-Vives C, Ferrer-Blasco T, et al. Device interchangeability on anterior chamber depth and white-to-white measurements: a thorough literature review. Int J Ophthalmol. 2016;9:1057–65.
67. Salouti R, Nowroozzadeh MH, Zamani M, Ghoreyshi M, Khodaman AR. Comparison of horizontal corneal diameter measurements using the Orbscan IIz and Pentacam HR systems. Cornea. 2013;32(11):1460–4.
68. Huang J, McAlinden C, Huang Y, Wen D, Savini G, Tu R, Wang Q. Metaanalysis of optical low-coherence reflectometry versus partial coherence interferometry biometry. Sci Rep. 2017;7:43414. Available at: https://www.ncbi.nlm.nih.gov/pmc/articles/PMC5324074/pdf/srep43414.pdf. Accessed 18 Mar 2021.
69. Teshigawara T, Meguro A, Mizuki N. Influence of pupil dilation on the Barrett universal II (new generation), Haigis (4th generation), and SRK/T (3rd generation) intraocular lens calculation formulas: a retrospective study. BMC Ophthalmol. 2020;20:299.
70. Arriola-Villalobos P, et al. Effect of pharmacological pupil dilation on measurements and IOL power calculation made using the new swept-source optical coherence tomography-based optical biometer. J Fr Ophtalmol. 2016;39:859.
71. Wang X, Dong J, Tang M. Effect of pupil dilation on measurements and intraocular lens power calculations in schoolchildren. PLoS One. 2018;13(9):e0203677.
72. Bakbak B, Koktekir BE, Gedik S. The effect of pupil dilation on biometric parameters of the Lenstar 900. Cornea. 2013;32:e21–4.
73. Huang J, McAlinden C, Su B. The effect of cycloplegia on the Lenstar and the IOLMaster biometry. Optom Vis Sci. 2012;89:1691–6.
74. Ferreira TB, Hoffer KJ, Ribeiro F, Ribeiro P, O'Neill JG. Ocular biometric measurements in cataract surgery candidates in Portugal. PLoS One. 2017;12(10):e0184837.
75. Wong TY, Foster PJ, Ng TP, Tielsch JM, Johnson GJ, Seah SK. Variations in ocular biometry in an adult Chinese population in Singapore: the Tanjong Pagar survey. Invest Ophthalmol Vis Sci. 2001;42:73–80.
76. Lege BA, Haigis W. Laser interference biometry versus ultrasound biometry in certain clinical conditions. Graefes Arch Clin Exp Ophthalmol. 2004;242:8–12.
77. Cao X, Hou X, Bao Y. The ocular biometry of adult cataract patients on lifeline express hospital eye train in rural China. J Ophthalmol. 2015;2015(5):171564.
78. Jivrajka R, Shammas MC, Boenzi T, Swearingen M, Shammas HJ. Variability of axial length, anterior chamber depth, and lens thickness in the cataractous eye. J Cataract Refract Surg. 2008;34:289–94.
79. Lee KE, Klein BK, Klein R, Quandt Z, Wong TY. Age, stature, and education associations with ocular dimensions in an older white population. Arch Ophthalmol. 2009;127:88–93.
80. Hoffer KJ. Axial dimension of the human cataractous lens. Arch Ophthalmol. 1993;111(7):914–8. Erratum 1993;111(12):1626.
81. Hoffmann PC, Hutz WW. Analysis of biometry and prevalence data for corneal astigmatism in 23,239 eyes. J Cataract Refract Surg. 2010;36(9):1479–85.
82. Ning X, Yang Y, Yan H, et al. Anterior chamber depth—a predictor of refractive outcomes after age-related cataract surgery. BMC Ophthalmol. 2019;19:134.
83. Gökce SE, Montes De Oca I, Cooke DL, Wang L, Koch DD, Al-Mohtaseb Z. Accuracy of 8 intraocular lens calculation formulas in relation to anterior chamber depth in patients with normal axial lengths. J Cataract Refract Surg. 2018;44:362–8.
84. Jeong J, Song H, Lee JK, Chuck RS, Kwon JW. The effect of ocular biometric factors on the accuracy of various IOL power calculation formulas. BMC Ophthalmol. 2017;17:62.
85. Yang S, Whang WJ, Joo CK. Effect of anterior chamber depth on the choice of intraocular lens calculation formula. PLoS One. 2017;12:e0189868.
86. Vega Y, Gershoni A, Achiron A, et al. High agreement between Barrett universal II calculations with and without utilization of optional biometry parameters. J Clin Med. 2021;10(3):542.
87. Jeong J, Song H, Lee JK, et al. The effect of ocular biometric factors on the accuracy of various IOL power calculation formulas. BMC Ophthalmol. 2017;17:62.
88. Hipólito-Fernandes D, Luís ME, Serras-Pereira R, Gil P, Maduro V, Feijão J, Alves N. Anterior chamber depth, lens thickness and intraocular lens calculation formula accuracy: nine formulas comparison. Br J Ophthalmol. 2020;106:349.
89. Fernández J, Rodríguez-Vallejo M, Poyales F, Burguera N, Garzón N. New method to assess the accuracy of intraocular lens power calculation formulas according to ocular biometric parameters. J Cataract Refract Surg. 2020;46(6):849–56.

90. Shrivastava AK, Behera P, Kacher R, Kumar B. Effect of anterior chamber depth on predictive accuracy of seven intraocular lens formulas in eyes with axial length less than 22 mm. Clin Ophthalmol. 2019;13:1579–86.
91. Weekers R, Delmarcelle Y, Luyckx J. Biometrics of the crystalline lens. In: Bellows JG, editor. Cataract and abnormalities of the lens. New York: Grune & Stratton; 1975. p. 134–47.
92. Farnsworth PN, Shyne SE. Anterior zonular shifts with age. Exp Eye Res. 1979;28(3):291–7.
93. Cook CA, Koretz JF, Pfahnl A, Hyun J, Kaufman PL. Aging of the human crystalline lens and anterior segment. Vis Res. 1994;34(22):2945–54.
94. Kim SY, Lee SH, Kim NR, Chin HS, Jung JW. Accuracy of intraocular lens power calculation formulas using a swept-source optical biometer. PLoS One. 2020;15(1):e0227638.
95. Eom Y, Song JS, Kim YY, Kim HM. Comparison of SRK/T and Haigis formulas for predicting corneal astigmatism correction with toric intraocular lenses. J Cataract Refract Surg. 2015;41:1650–7.
96. Symes RJ, Ursell PG. Automated keratometry in routine cataract surgery: comparison of Scheimpflug and conventional values. J Cataract Refract Surg. 2011;37(2):295–301.
97. http://acrysoftoriccalculator.com. Accessed 12 Jul 2018.
98. Savini G, Hoffer KJ, Ducoli P. A new slant on toric intraocular lens power calculation. J Refract Surg. 2013;29(5):348–54.
99. Savini G, Hoffer KJ, Carbonelli M, Ducoli P, Barboni P. Influence of axial length and corneal power on the astigmatic power of toric intraocular lenses. J Cataract Refract Surg. 2013;39:1900–3.
100. Savini G, Naeser K. An analysis of the factors influencing the residual refractive astigmatism after cataract surgery with toric intraocular lenses. Invest Ophthalmol Vis Sci. 2015;56:827–35.
101. Goggin M, Moore S, Easterman A. Outcome of toric intraocular lens implantation after adjusting for anterior chamber depth and intraocular lens sphere equivalent power effects. Arch Ophthalmol. 2011;129:998–1003; correction, 1494.
102. Fam HB, Lim KL. Meridional analysis for calculating the expected spherocylindrical refraction in eyes with toric intraocular lenses. J Cataract Refract Surg. 2007;33:2072–6.
103. Ribeiro F, Prata M, Mendanha DJ. Position measurement to improve refractive outcomes in cataract surgery. Adv Ophthalmol Vis Syst. 2016;4(3):84–5.
104. Goto S, Maeda N, Koh S, Ohnuma K, Hayashi K, Iehisa I, Noda T, Nishida K. Prediction of postoperative intraocular lens position with angle-to-angle depth using anterior segment optical coherence tomography. Ophthalmology. 2016;123(11):2474–80.
105. Martinez-Enriquez E, Pérez-Merino P, Durán-Poveda S, et al. Estimation of intraocular lens position from full crystalline lens geometry: toward a new generation of intraocular lens power calculation formulas. Sci Rep. 2018;8:9829.
106. Satou T, Shimizu K, Tsunehiro S, et al. Development of a new intraocular lens power calculation method based on lens position estimated with optical coherence tomography. Sci Rep. 2020;10:6501.
107. Li T, Yang K, Stein JD, Nallasamy N. Gradient boosting decision tree algorithm for the prediction of postoperative intraocular lens position in cataract surgery. Transl Vis Sci Technol. 2020;9(13):38.
108. Li T, Stein JD, Nallasamy N. AI-powered effective lens position prediction improves the accuracy of existing lens formulas. medRxiv. 2020; https://doi.org/10.1101/2020.10.29.20222539.